Acta Biochim Biophys Sin, 2015, 47(10), 767–774
doi: 10.1093/abbs/gmv079
Advance Access Publication Date: 3 September 2015
Original Article

Original Article

Inflammatory stress induces lipid accumulation in multi-organs of *db*/*db* mice

Kun Ling Ma*, Yang Zhang, Jing Liu, Yu Wu, Ze Bo Hu, Liang Liu, and Bi Cheng Liu

Institute of Nephrology, Zhong Da Hospital, Southeast University School of Medicine, Nanjing 210009, China

*Correspondence address. Tel/Fax: +86-25-83262442; E-mail: klma05@163.com

Received 6 February 2015; Accepted 21 May 2015

Abstract

Dyslipidemia and chronic inflammation play crucial roles in the progression of diabetes. This study aimed to investigate the effects of inflammatory stress on lipid accumulation in multi-organs in diabetes. Eight-week-old male *db*/*db* mice were randomly assigned to inflamed group with alternating day subcutaneous injection of 10% casein or control group with daily injection of distilled water. The lipid profile and plasma levels of inflammatory cytokines were determined using a clinical biochemical assay and enzyme-linked immunosorbent assay. The effects of inflammation on lipid accumulation in target organs were evaluated by hematoxylin–eosin staining, Oil Red O staining, Filipin staining, and a quantitative intracellular cholesterol assay. The protein expressions of low-density lipoprotein receptor (LDLr), sterol regulatory element binding protein-2 (SREBP-2), and SREBP-cleavage-activating protein (SCAP) in tissues were assessed by immunohistochemical staining and western blotting. Results showed that the serum levels of inflammatory cytokines were significantly elevated in casein-injected mice, suggesting that an inflamed diabetic model was established. Furthermore, the protein expressions of inflammatory cytokines in aortas, livers, kidneys, and intestines were significantly increased in inflamed group compared with control. Whereas the serum levels of lipid moieties in inflamed mice were not different compared with the control, inflammatory stress significantly increased lipid accumulation in aortas, livers, kidneys, and intestines, which coincided with increased protein expressions of LDLr, SREBP-2, and SCAP in these organs of inflamed mice. In conclusion, inflammation induces lipid accumulation in multi-organs of *db*/*db* mice from the circulation to peripheral tissues, potentially due to lipid redistribution mediated by the disruption of LDLr feedback regulation.

Key words: inflammatory stress, lipid accumulation, diabetes, LDL receptor, lipid redistribution

Introduction

Diabetes mellitus (DM) and its associated complications represent a public health problem that has reached epidemic proportions due to the rapidly increasing rates of DM throughout the world [1]. Both type 1 DM and type 2 DM (T2D) are associated with significantly accelerated rates of microvascular complications, such as diabetic nephropathy (DN), neuropathy, and retinopathy, and macrovascular cardiovascular diseases such as atherosclerosis, hypertension, and stroke [2]. However, the mechanisms responsible for the great risk of complications accompanying DM are multifaceted and still largely unknown.

Obesity and related metabolic abnormalities, such as inflammation and lipid disturbance, play a role in diabetic complications including atherosclerosis, nonalcoholic fatty liver disease (NAFLD), and DN. A growing number of studies have demonstrated that diabetes is a chronic inflammatory disease [3]. The atherosclerosis risk in communities study revealed that a mild state of inflammation precedes and predicts T2D, independent of other risk factors such as obesity [4].

Pickup and Crook [5] first proposed that long-term innate immune system activation results in chronic inflammation, elicits disease rather than repair and leads to the development of T2D. The mechanisms by which chronic inflammation can evoke T2D are not completely clear.

Dyslipidemia is one of the key risk factors for cardiovascular complications in patients with DM. It is important to note that dyslipidemia in diabetic patients is more artherogenic than that in nondiabetics [6]. The dyslipidemia that is associated with T2D and glucose intolerance consists of elevated triglycerides (TGs) and low high-density lipoprotein cholesterol (HDL-C), whereas low-density lipoprotein cholesterol (LDL-C) levels are generally similar to those observed in nondiabetic patients [7].

In patients with diabetes, alterations in lipid distribution increase the risk of atherosclerosis. It is well known that the LDL receptor (LDLr) pathway is a feedback system with important functions in regulating both plasma and intracellular cholesterol homeostasis. Our previous studies demonstrated that inflammatory stress exacerbates lipid accumulation in hepatic and vascular smooth muscle cells and accelerates the progression of NAFLD and atherosclerosis by disrupting LDLr feedback regulation [8–10]. Therefore, this study aimed to investigate the effects of inflammation on lipid accumulation in multi-organs in DM and to explore its underlying mechanisms.

Materials and Methods

Animal model

Eight-week-old male diabetic *db*/*db* mice (weighing 33–43 g) on a C57BL/KsJ genetic background were purchased from the Model Animal Centre of Nanjing University (Nanjing, China). Animal experiment protocols were approved by the Ethical Committee of Southeast University following the latest version of the Declaration of Helsinki. Mice fed with a normal chow diet containing 4% fat were randomly assigned to inflamed group with alternating day subcutaneous injections of 0.5 ml of 10% casein (Sigma, St Louis, USA) or control group with daily injections of 0.5 ml of distilled water for 8 weeks ($n = 10$). Mice were placed separately in metabolic cages for 24-h urine collection. At the end of the experimental period, blood samples were obtained from the right ventricle for biochemical assays and to determine the serum levels of inflammatory cytokines. The samples from aortas, livers, kidneys, and intestines were used for histological assessments.

Biochemical assays

The concentrations of blood glucose (BG), blood urea nitrogen, serum creatinine (Scr), urine creatinine, TG, total cholesterol (TC), HDL, and LDL were determined using a Hitachi 7600-110 Automatic Analyzer (Hitachi, Tokyo, Japan). The quantitative analysis of 24-h urinary protein was determined using Lowry method. The serum levels of amyloid protein A and tumor necrotic factor-α (TNF-α) were measured by enzyme-linked immunosorbent assay using SAA kit (Invitrogen, Carlsbad, USA) and TNF-α kit (R&D, Minneapolis, USA), respectively.

Hematoxylin–eosin staining

Paraffin-embedded aorta, liver, kidney, and intestine samples were sectioned and dewaxed. Sections were stained for 15 min with hematoxylin, followed by staining with 1% eosin for 3 min. After dehydration, resimene was used to seal the sections to transparency. The sections were observed under a light microscope (Olympus, Tokyo, Japan).

Observation of lipid accumulation

The lipid accumulation in aortas, livers, kidneys, and intestines of *db*/*db* mice was evaluated by Oil Red O (Sigma) and Filipin staining (Genmed, Shanghai, China). Briefly, samples were fixed with 5% formalin solution and then stained with Oil Red O for 30 min. Finally, the samples were counterstained with hematoxylin for 5 min. The results were examined by light microscopy. For Filipin staining, samples were fixed with 4% paraformaldehyde for 30 min, washed with phosphate-buffered saline (PBS) and incubated with freshly prepared Filipin solution for 30 min. Then, slides were washed with PBS, and a drop of phenylenediamine/glycerol was added. The slides were then mounted with coverslips and examined by confocal laser scanning microscopy. The values of semiquantitative analysis for the Filipin positive areas were quantified by the software of Image-Pro Plus version 6.0.

Quantitative measurement of intracellular cholesterol

Quantitative measurement of intracellular total and free cholesterol was analyzed using the method described by Gamble *et al.* [11]. In brief, liver, kidney, and intestine samples were collected, and the lipids were extracted with 1 ml of chloroform/methanol (2:1). The lipid phase was collected, dried in vacuum, and then dissolved in 2-propanol containing 10% Triton X-100. The concentration of total and free cholesterol was analyzed using a standard curve and normalized by total protein from tissue lysates. The concentration of cholesteryl ester was calculated by subtracting free cholesterol from TC.

Immunohistochemistry

Paraffin-embedded sections (3 μm) were subject to immunohistochemical examination. After deparaffinization, sections were placed in citrate-buffered solution (pH 6.0) and heated for antigen retrieval. Endogenous peroxidase activity was blocked with 3% hydrogen peroxide treatment, and nonspecific binding was blocked with normal nonimmune serum. Subsequently, the sections were incubated with anti-mouse primary antibodies against TNF-α, monocyte chemotactic protein-1 (MCP-1), LDLr, sterol regulatory element binding protein-2 (SREBP-2), and SREBP-cleavage-activating protein (SCAP) (Santa Cruz, Dallas, USA) overnight at 4°C, followed by incubation with biotinylated secondary antibodies. Finally, a diaminobenzidine tetrahydrochloride substrate was used to develop the reaction. The results were observed under a light microscope. Semiquantitative analysis was performed by the software of Image-Pro Plus version 6.0.

Western blot analysis

Equal amounts (70 μg) of total protein from the liver and kidney homogenates of *db*/*db* mice were separated by (5%) sodium dodecyl sulfate polyacrylamide gel electrophoresis and then transferred onto polyvinylidene fluoride (PVDF) membranes. The membranes were blocked with 5% skim milk in Tris-buffered saline containing 0.5% Tween 20 for 1 h at room temperature. The membranes were then incubated with anti-mouse primary antibodies against MCP-1, TNF-α, LDLr, SCAP, and SREBP-2 overnight at 4°C, followed by incubation with horseradish peroxidase-labeled secondary antibodies for 2 h. β-Actin was used as an internal sample loading control and was detected with a mouse monoclonal anti-β-actin antibody (Santa Cruz). Finally, signals were detected using an enhanced chemiluminescence kit (GE Healthcare, Pittsburgh, USA). Relative expression levels were determined by normalization against β-actin.

Statistical analysis

Data were expressed as the mean ± SD and were processed using the SPSS software 16.0 (IBM, USA). Continuous variables were compared between the groups with an independent-sample *t* test (where appropriate). The differences were considered significant if the *P* value was <0.05.

Results

Basic biochemical data in two groups of mice

As shown in Table 1, BG and Scr were significantly increased and creatinine clearance rate (Ccr) was significantly decreased in the inflamed group compared with those in the control group ($P < 0.01$). There were no significant differences in TG, TC, LDL, and HDL levels between the inflamed group and the control group.

Increased levels of inflammatory cytokines in plasma, aortas, livers, kidneys, and intestines

To check whether an inflamed DM model was established successfully, the serum levels of SAA and TNF-α were measured. It was shown that the levels of serum SAA (**Fig. 1A**) and TNF-α (**Fig. 1B**) were significantly increased in the casein-injected mice compared with the control group, suggesting that systemic inflammation was successfully induced. To observe the local change of inflammation in the target organs, we examined the protein expressions of inflammatory cytokines by immunohistochemical staining and western blotting. It was found that there were increased protein expressions of MCP-1 (**Fig. 2A,B**) and TNF-α (**Fig. 2C, D**) in the aortas, livers, kidneys, and intestines of the inflamed group compared with the control. The results were further confirmed by western blot analysis in kidney and liver (**Fig. 2E,F**). These findings indicated that local inflammation in peripheral tissues was activated.

Table 1. Basic biochemical data of the two groups of mice

Parameters	Control group	Inflamed group
BG (mM)	46.47 ± 3.90	52.42 ± 4.30*
TG (mM)	1.22 ± 0.27	1.17 ± 0.29
TC (mM)	3.36 ± 0.17	3.32 ± 0.13
LDL (mM)	1.03 ± 0.09	1.37 ± 0.11
HDL (mM)	1.58 ± 0.18	1.23 ± 0.09
BUN (mM)	11.70 ± 1.10	13.70 ± 5.33
Scr (mM)	17.33 ± 2.31	24.00 ± 6.93*
Ccr (ml/min)	0.387 ± 0.053	0.250 ± 0.025*

Eight-week-old male diabetic *db/db* mice fed with a normal chow diet containing 4% fat were randomly assigned to alternating day subcutaneous injections of 0.5 ml of 10% casein (inflamed group) or daily injections of 0.5 ml of distilled water (control group) for 8 weeks ($n = 10$).

BG, blood glucose; TG, triglyceride; TC, total cholesterol; LDL, low-density lipoprotein; HDL, high-density lipoprotein; BUN, blood urea nitrogen; Scr, serum creatinine; Ccr, creatinine clearance rate.

*$P < 0.05$ vs. control group.

Inflammatory stress induces lipid accumulation in aortas, livers, kidney, and intestines and exacerbates histopathological damage in *db/db* mice

To explore the effect of inflammation on the lipid accumulation in *db/db* mice, we checked the foam cell formation and lipid content change in different issues. Interestingly, hematoxylin–eosin (HE) staining (**Fig. 3A**) showed significant foam cell formation in the aortas, livers, and intestines of the inflamed group compared with the controls. Oil Red O (**Fig. 3B**) and Filipin staining (**Fig. 3C,D**) results demonstrated that inflammation significantly increased lipid droplets in the aortas, livers, kidneys, and intestines in the inflamed group compared with the controls. The quantitative analysis of intracellular cholesterol further confirmed the results from Oil Red O and Filipin staining (**Fig. 3E**). These findings suggest that inflammatory stress may induce lipid redistribution from the plasma to peripheral tissues.

Inflammation disrupts LDL receptor feedback regulation

To explore the potential mechanisms of this phenomenon, we investigated the effects of inflammation on the LDLr pathway in these tissues. Immunohistochemical staining and western blotting were used to observe the expression of LDLr pathway-related proteins, including LDLr, SREBP-2, and SCAP. The results showed that inflammation significantly increased LDLr, SCAP, and SREBP-2 protein expressions in aorta (**Fig. 4A,B**), liver (**Fig. 4C,D**), kidney (**Fig. 4E,F**), and intestine (**Fig. 4G,H**). And the results of western blot analysis in kidney and liver showed that the protein expression levels of LDLr, SCAP, and SREBP-2 were also significantly increased in the inflamed group (**Fig. 4I,J**). These findings were in agreement with those from immunohistochemical staining, suggesting that lipid redistribution may be mediated through the inflammatory stress-induced disruption of the LDLr pathway.

Discussion

Diabetic patients commonly show dyslipidemia, which is strongly associated with an increased risk for macrovascular events [12].

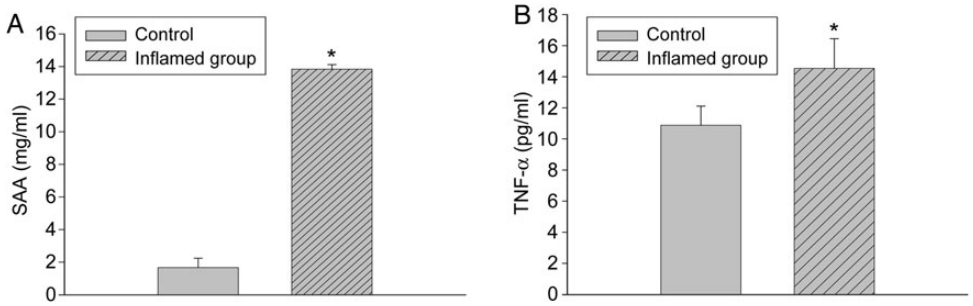

Figure 1. The plasma levels of inflammatory cytokines in two groups of mice Eight-week-old male diabetic *db/db* mice fed a normal chow diet containing 4% fat were randomly assigned to alternating day subcutaneous injections of 0.5 ml of 10% casein (inflamed group) or daily injections of 0.5 ml of distilled water (control group) for 8 weeks ($n = 10$). The levels of SAA (A) and TNF-α (B) in the serum were measured by ELISA. The results are presented as the mean ± SD. *$P < 0.01$ vs. control.

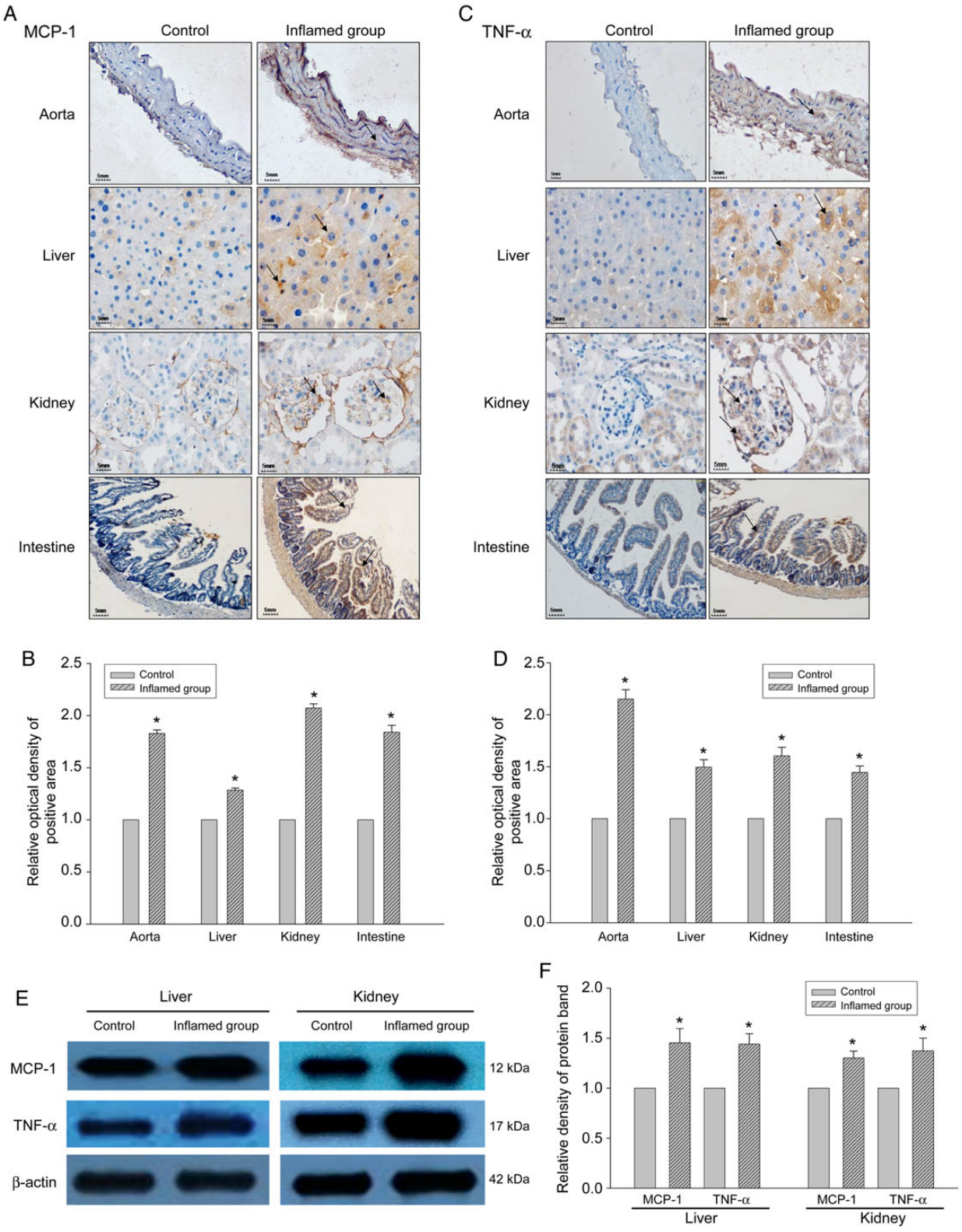

Figure 2. Inflammatory stress increases the protein expressions of inflammatory cytokines in the aortas, livers, kidneys, and intestines of *db*/*db* mice
Eight-week-old male diabetic *db*/*db* mice fed a normal chow diet containing 4% fat were randomly assigned to alternating day subcutaneous injections of 0.5 ml of 10% casein (inflamed group) or daily injections of 0.5 of ml distilled water (control group) for 8 weeks ($n = 10$). The protein expressions of TNF-α and MCP-1 in the aortas, livers, kidneys, and intestines were measured by immunohistochemical staining. The values of semiquantitative analysis for the positive areas were expressed as the mean ± SD in each group, $^*P < 0.05$ vs. control. (A–D) Brown staining shown by arrows indicates areas of positive protein expression. Original magnification, 400×. (E, F) Western blot analysis. The histogram represents the mean ± SD of the densitometric scans for TNF-α and MCP-1 protein bands from the mice group, normalized to β-actin, and expressed as the percentage of the control. $^*P < 0.01$ vs. control.

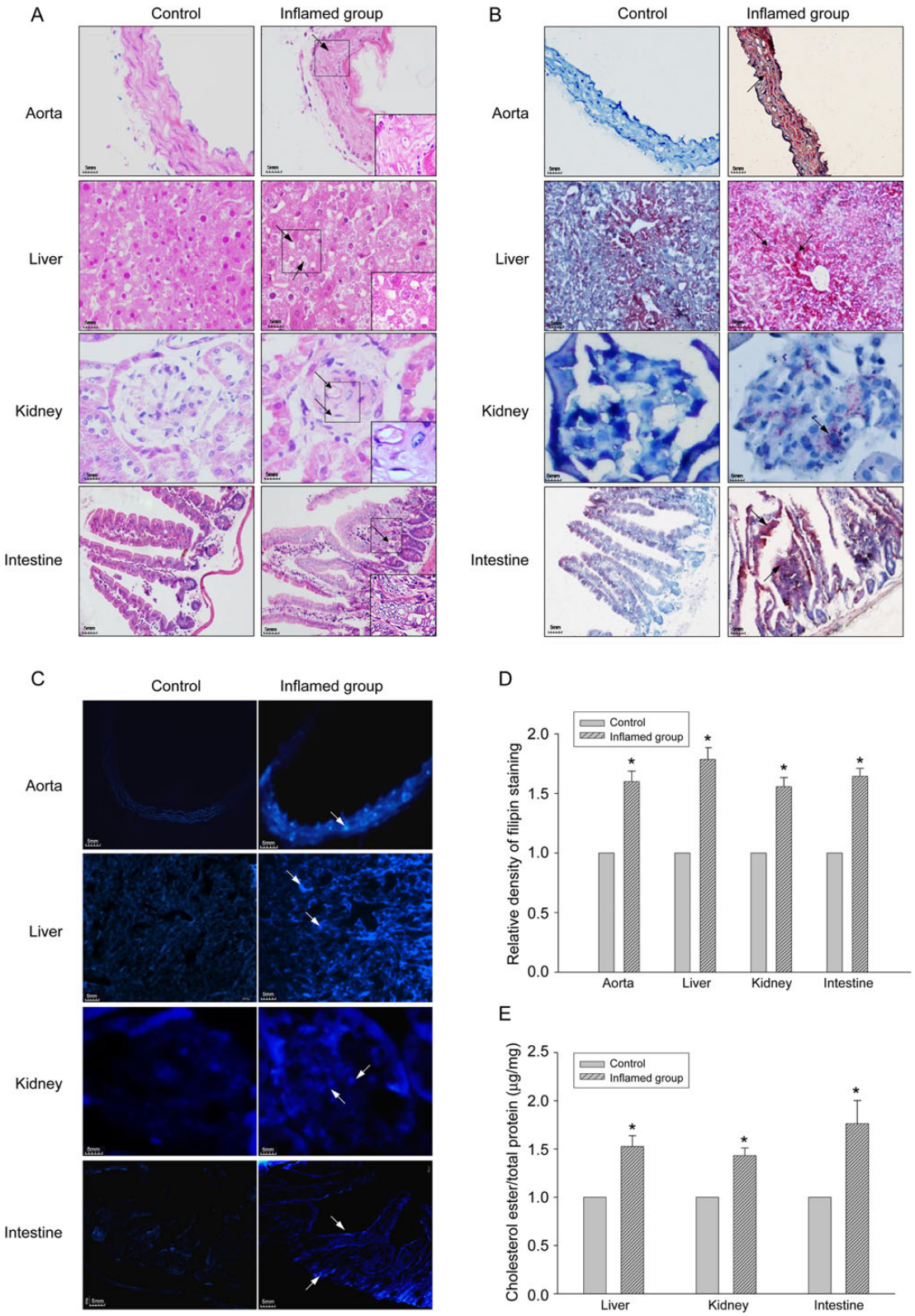

Figure 3. Inflammatory stress induces lipid accumulation in the aortas, livers, kidneys, and intestines in *db*/*db* mice Eight-week-old male diabetic *db*/*db* mice fed with a normal chow diet containing 4% fat were randomly assigned to alternating day subcutaneous injections of 0.5 ml of 10% casein (inflamed group) or daily injections of 0.5 ml of distilled water (control group) for 8 weeks ($n = 10$). The histopathological changes were assessed by HE staining (A, the arrows show fat vacuoles, original magnification 400×). The tissues were examined for lipid accumulation by Oil Red O and Filipin staining (B–D, the arrows show cholesterol accumulation, original magnification 400×). The values of semiquantitative analysis for the Filipin positive areas were expressed as the mean ± SD in each group. *$P < 0.05$ vs. control. The concentration of cholesteryl ester in livers, kidneys, and intestine was measured (E) and results are presented as the mean ± SD. *$P < 0.01$ vs. control.

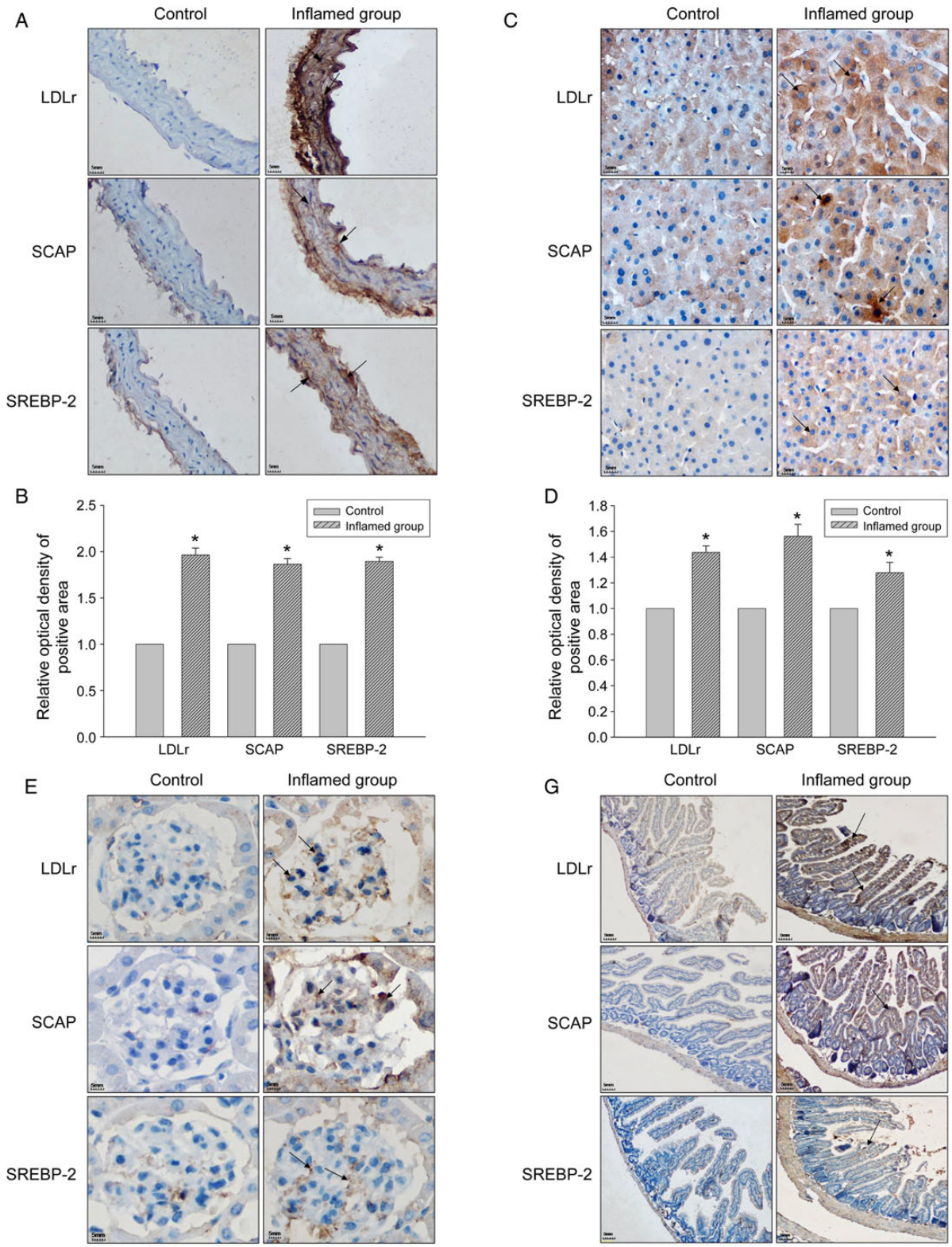

Figure 4. Inflammatory stress disrupts the feedback regulation of LDLr pathway in the aortas, livers, kidneys, and intestines of *db*/*db* mice Eight-week-old male diabetic *db*/*db* mice fed with a normal chow diet containing 4% fat were randomly assigned to alternating day subcutaneous injections of 0.5 ml of 10% casein (inflamed group) or daily injections of 0.5 ml of distilled water (control group) for 8 weeks ($n = 10$). The protein expression of LDLr, SCAP, and SREBP-2 in the aortas (A, B), livers (C, D), kidneys (E, F), and intestines (G, H) was measured by immunohistochemical staining. Brown staining shown by arrows indicates areas of positive protein expression. Original magnification, 400×. The values of semiquantitative analysis for the positive areas were expressed as the mean ± SD in each group. * $P < 0.05$ vs. control. (I and J) Western blot analysis. The histogram represents the mean ± SD of the densitometric scans for LDLr, SCAP, and SREBP-2 protein bands from each group, normalized to β-actin and expressed as the percentage of control. * $P < 0.05$ vs. control.

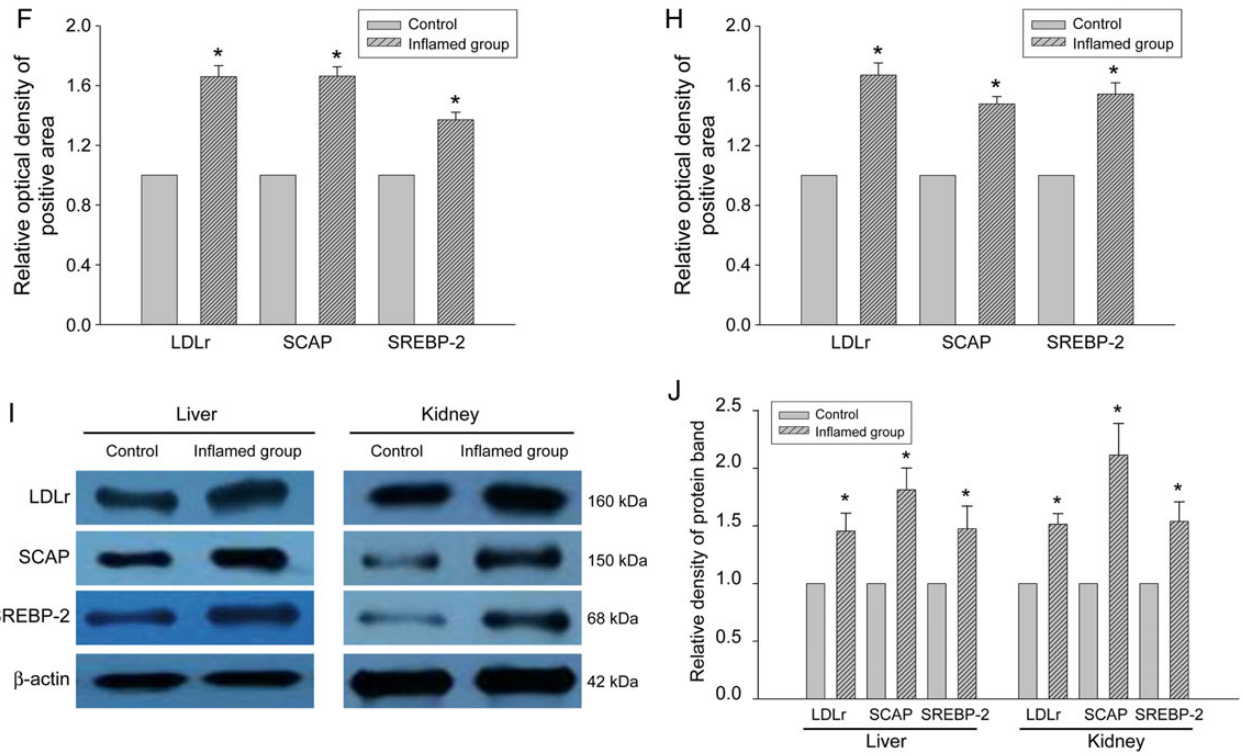

Figure 4 Continued

A systematic review of studies assessing associations between lipid subfractions and macrovascular events revealed that dyslipidemia may cause or exacerbate diabetes and its complications [13].

Under physiological conditions, excessive free fatty acid is converted to TG or cholesteryl ester to be stored in adipocyte lipid droplets [14]. The initial deposition of TGs occurs in subcutaneous adipose tissue, and as the deposition increases in size, insulin resistance increases, which limits further subcutaneous lipid accumulation [15]. Lipids are then diverted to visceral fat depots and nonadipose tissue, which is also known as ectopic lipid accumulation or lipid redistribution [16,17]. Lipid redistribution may occur at several levels and sites: from circulation to tissue, from tissue to tissue, and from organelle to organelle [18]. Therefore, plasma levels of LDL cholesterol in patients might be a poor marker for the risk of lipid-mediated organ injuries. The factors affecting lipid redistribution include chronic inflammation [18], decreased glomerular filtration rate [18], activation of the renin–angiotensin system [19,20], insulin resistance, and drug administration (e.g. steroids and rapamycin) [10].

Recently, the role of chronic inflammation in lipid redistribution has become a popular subject of research. Inflammation and lipid disorders are 'partners in crime' [21]. It is becoming clear that inflammation is a major contributor to the development and progression of atherosclerosis, NAFLD, chronic kidney disease, and DM. When persistent, inflammation may play a major role in aggravating lipid disorder-mediated organ injuries. Our results showed that the serum levels of inflammatory cytokines and their expression in target organs were significantly increased in casein-injected *db*/*db* mice compared with the controls, suggesting that an inflamed DM animal model was successfully established [22]. Furthermore, significantly increased levels of BG and Scr, but diminished level of Ccr in casein-injected *db*/*db* mice suggested that inflammatory stress exacerbated the progression of DN.

It is well known that most tissues have a small intracellular reserve of lipids. These reserves serve as an immediate energy source and a foundation for essential 'housekeeping' functions such as the maintenance of membrane structure, fluidity, and intracellular signaling [16]. In some cases, the disruption of such classic regulatory pathways will lead to cell dysfunction and lipid deposition into other nonadipose organs, such as the liver, intestine, arteries, and kidneys. Therefore, we further observed the effects of inflammation on lipid accumulation in the aortas, livers, kidneys, and intestines of the *db*/*db* mice. It was found that chronic inflammation contributed to lipid accumulation and foam cell formation in these target organs with more severe tissue damage. These results suggested that inflammatory stress may induce lipid redistribution from the circulation to target tissues, thereby aggravating the progression of diabetes and its complications.

Lipid accumulation in the peripheral tissues of inflamed *db*/*db* mice means that intracellular dynamic cholesterol homeostasis is disrupted, which may be correlated with the dysregulation of lipoprotein receptor-mediated cholesterol influx or efflux, such as the LDLr pathway, which modulates cholesterol uptake. Physiologically, LDLr expression is predominantly regulated by the intracellular cholesterol pool at the transcriptional level through a negative feedback mechanism. An elevated intracellular concentration of cholesterol prevents the transport of SCAP/SREBP-2 complexes from the endoplasmic reticulum to the Golgi, thereby down-regulating LDLr expression [23]. To explore the potential mechanisms underlying lipid redistribution, we further assessed the effects of inflammatory stress on the LDLr pathway in inflamed *db*/*db* mice. Our results showed that the protein expressions of LDLr, SCAP, and SREBP-2 were significantly increased in the aortas, livers, kidneys, and intestines in inflamed *db*/*db* mice compared with controls. This finding suggested that the disruption of the LDLr pathway induced by inflammation might be involved in the lipid redistribution of inflamed *db*/*db* mice. These findings were in

agreement with our previous results from *in vivo* and *in vitro* studies which demonstrated that chronic inflammation exacerbates lipid accumulation in aortas, livers, and kidneys, whereas anti-inflammatory strategies showed beneficial effects [8–10,24–26]. Our previous studies in different inflamed animal models verified a lipid redistribution pattern driven by inflammation and provided a reasonable explanation for the phenomena of reverse epidemiology occurring in hemodialysis patients: a lower plasma cholesterol level indicates a greater risk of cardiovascular disease [27,28].

In summary, our study, for the first time, demonstrated that inflammatory stress induces lipid redistribution from the circulation to peripheral tissues by disrupting the LDLr pathway in diabetic mellitus, which accelerates the progression of atherosclerosis, glomerulosclerosis, and fatty liver. Moreover, our findings provide experimental evidence for the treatment of clinical DM patients with microinflammation. During an inflammatory state, the serum lipid concentrations in these patients are poor biomarkers for the diagnosis of lipid disorder-mediated organ injuries. Therefore, anti-inflammatory therapy combined with lipid-modulating therapy could be a promising clinical treatment.

Funding

This work was supported by the grants from the National Natural Science Foundation of China (Nos. 81170792, 81070571, and 81470957), the Natural Science Foundation of Jiangsu Province (No. BK20141343), and the Clinical Medical Science and Technology Special Project of Jiangsu Province (No. BL2014080).

References

1. El-Abhar HS, Schaalan MF. Phytotherapy in diabetes: review on potential mechanistic perspectives. *World J Diabetes* 2014, 5: 176–197.
2. Reagan LP. Diabetes as a chronic metabolic stressor: causes, consequences and clinical complications. *Exp Neurol* 2012, 233: 68–78.
3. Navarro JF, Mora C. Diabetes, inflammation, proinflammatory cytokines, and diabetic nephropathy. *Sci World J* 2006, 6: 908–917.
4. Luft VC, Schmidt MI, Pankow JS, Couper D, Ballantyne CM, Young JH, Duncan BB. Chronic inflammation role in the obesity-diabetes association: a case-cohort study. *Diabetol Metab Syndr* 2013, 5: 31.
5. Pickup JC, Crook MA. Is type II diabetes mellitus a disease of the innate immune system? *Diabetologia* 1998, 41: 1241–1248.
6. Mullugeta Y, Chawla R, Kebede T, Worku Y. Dyslipidemia associated with poor glycemic control in type 2 diabetes mellitus and the protective effect of metformin supplementation. *Indian J Clin Biochem* 2012, 27: 363–369.
7. Assmann G, Schulte H. Identification of individuals at high risk for myocardial infarction. *Atherosclerosis* 1994, 110: S11–S21.
8. Ma KL, Ruan XZ, Powis SH, Chen Y, Moorhead JF, Varghese Z. Inflammatory stress exacerbates lipid accumulation in hepatic cells and fatty livers of apolipoprotein E knockout mice. *Hepatology* 2008, 48: 770–781.
9. Ma KL, Liu J, Wang CX, Ni J, Zhang Y, Wu Y, Lv LL, *et al*. Activation of mTOR modulates SREBP-2 to induce foam cell formation through increased retinoblastoma protein phosphorylation. *Cardiovasc Res* 2013, 100: 450–460.
10. Ma KL, Ruan XZ, Powis SH, Moorhead JF, Varghese Z. Antiatherosclerotic effects of sirolimus on human vascular smooth muscle cells. *Am J Physiol Heart Circ Physiol* 2007, 292: H2721–H2728.
11. Gamble W, Vaughan M, Kruth HS, Avigan J. Procedure for determination of free and total cholesterol in micro- or nanogram amounts suitable for studies with cultured cells. *J Lipid Res* 1978, 19: 1068–1070.
12. Krauss RM. Lipids and lipoproteins in patients with type 2 diabetes. *Diabetes Care* 2004, 27: 1496–1504.
13. Steinmetz A. Treatment of diabetic dyslipoproteinemia. *Exp Clin Endocrinol Diabetes* 2003, 111: 239–245.
14. Beckman M. Cell biology. Great balls of fat. *Science* 2006, 311: 1232–1234.
15. Ali AT, Ferris WF, Naran NH, Crowther NJ. Insulin resistance in the control of body fat distribution: a new hypothesis. *Horm Metab Res* 2011, 43: 77–80.
16. Rasouli N, Molavi B, Elbein SC, Kern PA. Ectopic fat accumulation and metabolic syndrome. *Diabetes Obes Metab* 2007, 9: 1–10.
17. van Herpen NA, Schrauwen-Hinderling VB. Lipid accumulation in non-adipose tissue and lipotoxicity. *Physiol Behav* 2008, 94: 231–241.
18. Ruan XZ, Varghese Z, Moorhead JF. An update on the lipid nephrotoxicity hypothesis. *Nat Rev Nephrol* 2009, 5: 713–721.
19. Ma KL, Ni J, Wang CX, Liu J, Zhang Y, Wu Y, Lv LL, *et al*. Interaction of RAS activation and lipid disorders accelerates the progression of glomerulosclerosis. *Int J Med Sci* 2013, 10: 1615–1624.
20. Ni J, Ma KL, Wang CX, Liu J, Zhang Y, Lv LL, Ni HF, *et al*. Activation of renin-angiotensin system is involved in dyslipidemia-mediated renal injuries in apolipoprotein E knockout mice and HK-2 cells. *Lipids Health Dis* 2013, 12: 49.
21. Steinberg D. Atherogenesis in perspective: hypercholesterolemia and inflammation as partners in crime. *Nat Med* 2002, 8: 1211–1217.
22. Ma KL, Zhang Y, Liu J, Wu Y, Hu ZB, Ruan XZ, Liu BC. Establishment of an inflamed animal model of diabetic nephropathy. *Int J Biol Sci* 2014, 10: 149–159.
23. Nohturfft A, DeBose-Boyd RA, Scheek S, Goldstein JL, Brown MS. Sterols regulate cycling of SREBP cleavage-activating protein (SCAP) between endoplasmic reticulum and Golgi. *Proc Natl Acad Sci USA* 1999, 96: 11235–11240.
24. Ma KL, Varghese Z, Ku Y, Powis SH, Chen Y, Moorhead JF, Ruan XZ. Sirolimus inhibits endogenous cholesterol synthesis induced by inflammatory stress in human vascular smooth muscle cells. *Am J Physiol Heart Circ Physiol* 2010, 298: H1646–H1651.
25. Ma KL, Liu J, Gao M, Wang CX, Ni J, Zhang Y, Zhang XL, *et al*. Activation of mTOR contributes to foam cell formation in the radial arteries of patients with end-stage renal disease. *Clin Nephrol* 2014, 81: 396–404.
26. Ruan XZ, Varghese Z, Powis SH, Moorhead JF. Dysregulation of LDL receptor under the influence of inflammatory cytokines: a new pathway for foam cell formation. *Kidney Int* 2001, 60: 1716–1725.
27. Liu Y, Coresh J, Eustace JA, Longenecker JC, Jaar B, Fink NE, Tracy RP, *et al*. Association between cholesterol level and mortality in dialysis patients: role of inflammation and malnutrition. *JAMA* 2004, 291: 451–459.
28. Lowrie EG, Lew NL. Death risk in hemodialysis patients: the predictive value of commonly measured variables and an evaluation of death rate differences between facilities. *Am J Kidney Dis* 1990, 15: 458–482.